Rev. Adv. Mater. Sci. 33 (2013) 56-60

FABRICATION OF NANOPOROUS COPPER RIBBONS BY DEALLOYING OF $Mn_{70}Cu_{30}$ ALLOY AND FRACTAL CHARACTERIZATION OF THEIR POROSITY

Mei Li, Haoran Geng, Yongzhi Zhou and Liuwei Ding

School of Materials Science and Engineering, University of Jinan, Jinan 250022, P. R. China

Received: October 17, 2011

Abstract. Nanoporous copper (NPC) ribbons were synthesized by free corrosion dealloying in a 6 wt.% HCl solution for different corrosion times with $Mn_{70}Cu_{30}$ alloy ribbons prepared by single-roller melt spinning processing equipment for precursor samples. The microstructures and components of NPC were characterized by utilizing FE-SEM and EDS analysis. Additionally, 2-value digital image technique was used to process FE-SEM images, and porous structures of copper ribbons were quantitative characterized by fractal theory. The results showed that Mn was selectively dissolved from $Mn_{70}Cu_{30}$ alloy ribbons in HCl solution, and prepared NPC was uniform network-like structure, with the average ligament size of 114-214 nm and the average pore size in the range of 325-520 nm for different corrosion time. Porous structure of NPC is of typical fractal characteristic with fractal dimension in the range of 1.59-1.74. Fractal dimension reflects the heterogeneity of porous structure, thus, porosity of NPC can be characterized by fractal dimension.

1. INTRODUCTION

Due to the presence of many technological applications including catalysis, sensors, actuators and fuel cells [1-4], nanoporous metals with high surface areas and low density have attracted more attention. Nanoporous metals with nanosize pores and ligaments can be fabricated by chemical dealloying (or electrochemically etching) binary A_xB_{1-x} alloys [5]. In dealloying, a less noble element selectively dissolves from a binary alloy, and the remaining more noble element self-organizes an open-cell nanoporous structure. Recently, most attention has been paid to the dealloying of the prototypical Ag–Au system which results in the formation of nanoporous gold (NPG), and researchers have focused on the properties and applications of the NPG [6-8].

In order to fabricate homogenous, bicontinuous and porous structure by dealloying method, the starting alloy must be complete single-phase solid solution. Additionally, the standard electrode potentials of alloying elements are different enough to allow the selective removal of one constituent. The most suitable candidate is Mn-Cu for Cu alloy system. It has been previously shown that porous structure can be created by dealloying Mn–Cu, for instance, Hayes et al. [9] reported that monolithic nanoporous copper (NPC) could be synthesized by dealloying $Mn_{70}Cu_{30}$ by two distinct methods: potentiostatically driven dealloying and free corrosion. However, less attention has been paid to the porosity and fractal characterization of NPC. For complex and disordered materials, the traditional analytical methods can not fully and accurately characterize their properties.

Fractal theory has contributed significantly in the characterization of the distribution of physical or other quantities on a geometric support. It was proposed by Mandelbrot in the 1970s, and expanded by Lin (1982) to many other contexts [10]. Fractal geometry

Corresponding author: Haoran Geng, e-mail: limei8018@163.com

supplies a versatile and powerful theoretical framework to describe complex systems, which have been successfully applied to the quantitative description of microstructures such as surface roughness and amorphous metal structure. Fractal dimension is a parameter to quantitatively describe the structure of irregular geometric graph. Therefore, fractal theory provides a new and effective method for the complex structure of the porous material.

2. EXPERIMENTAL AND COMPUTING PROCEDURE

$Mn_{70}Cu_{30}$ alloy was produced from Cu and Mn of 99.99% purity by melting in an arc furnace. Then, the Mn-Cu ingot was remelted in a quartz tube by high-frequency induction heating and melt-spun onto a copper roller at a speed of 2000 r/min by utilizing a single-roller melt spinning system. In order to test the influence of corrosion time on the dealloying of $Mn_{70}Cu_{30}$ ribbons and formation of nanoporous copper (NPC), the dealloying of the $Mn_{70}Cu_{30}$ ribbons was performed in a 6 wt.% HCl aqueous solution for 2, 5, 8, 11, 14, and 17h, respectively, at room temperature. After being dealloyed, the samples were removed from the etching solution and placed in distilled water and dehydrated alcohol to displace the acid solution from the internal pores. Finally, the as-dealloyed samples were kept in a vacuum chamber to avoid oxidation.

The dealloyed samples and melt-spun $Mn_{70}Cu_{30}$ alloy were observed using a field emission scanning electron microscope (FE-SEM) with an energy dispersive X-ray (EDS) analyzer. Image Pro-Plus image was used to count the average ligament size and pore size. Additionally, 2-value digital image technique was used to process FE-SEM images, and porous structures of copper ribbons were quantitative characterized by fractal theory.

Fractalyse developed by Gilles Vuidel was used to measure fractal dimension of NPC's surface morphologies. Counting method goes step by step following an iteration principle. At each iteration step, the method involved counting the number of black pixels contained in a counting window. From one step to the next, the size of the counting window is enlarged. By doing that, we artificially change the level of analysis of the image. So, for each method we have two elements varying according to the counting step (iteration step)(i): the number of counted elements (which is roughly the number of black pixels present in the window) (N), the size of either the counting window (ε). Then, we obtain a series of points that can be represented on a 2-value FE-SEM graph. The Y-axis corresponds to the number of counted elements (N) and the X-axis corresponds to the size of the counting window ε, with ε increasing from step to step. Mathematically, the series of points is a curve (named the empirical curve). The next stage is to fit this empirical curve with another one, the estimated curve. If the empirical curve follows a fractal law, the estimated curve has the form of a power law (parabolic or hyperbolic), and D represents the fractal dimension.

$$N = \varepsilon^{D} \quad \text{or} \quad N = \varepsilon^{-D}. \tag{1}$$

For correlation method, each point of the image is surrounded with a small squared window. The number of occupied points inside each window is enumerated. This allows the mean number of points per window of that given size to be calculated. The same operation is applied for windows of increasing sizes. In principle it is possible to choose any shape for the window, such as circle, hexagon, etc. However, since pixels are square-like, the choice of a square helps to avoid rounding errors.

3. RESULTS AND DISCUSSIONS

According to Cu-Mn binary phase diagram, the phase constitution in equilibrium is a single (Cu, γ Mn) solid solution for the $Mn_{70}Cu_{30}$ alloy. Fig. 1(a–f) shows the network-like structure of as-dealloyed samples obtained by dealloying $Mn_{70}Cu_{30}$ in a 6 wt.% HCl for 2, 5, 8, 11, 14, and 17 h, respectively. The FE-SEM results confirm that nanoporous copper (NPC) can be obtained through dealloying of (Cu, γ Mn) solid solution in the acidic solution. This is very clear, in addition to the two hours and seventeen hours of corrosion samples, all NPC samples exhibit an open, three-dimensional bicontinuous interpenetrating ligament–channel structure with nanometer length scales. Moreover, the ligament size and pore size in NPC changed slightly with increasing corrosion time. Fig. 1 also shows the evolution of porous structure in corrosion process. Initially, manganese atoms are dissolved from surface sites, leaving behind a large number of copper atoms with no coordinationatom. Because of having high liquidity, these copper atoms can spread around to gather into metal clusters, thus the formation of the structure is shown in Fig. 1a. At that time, obviously, the as-dealloyed ribbons were not completely corroded, and porosity only formed on the surface. Moreover, EDS results also demonstrate that some of residual Mn can be detected in the NPC samples obtained. Then, with further corrosion of manganese and agglomeration

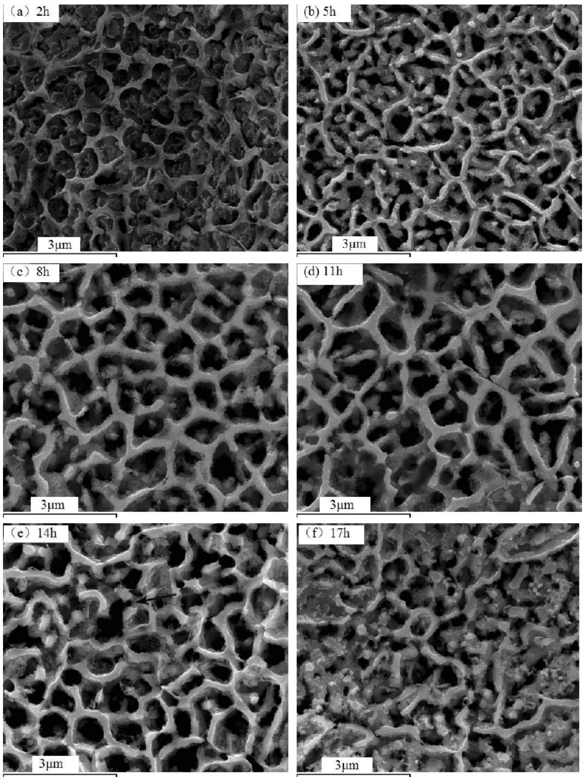

Fig. 1. FE-SEM images showing the microstructure of NPC by dealloying of $Mn_{70}Cu_{30}$ alloy in a 6 wt.% HCl solution with different corrosion times: (a) 2 h, (b) 5h, (c) 8h, (d) 11h, (e) 14h, and (f) 17h.

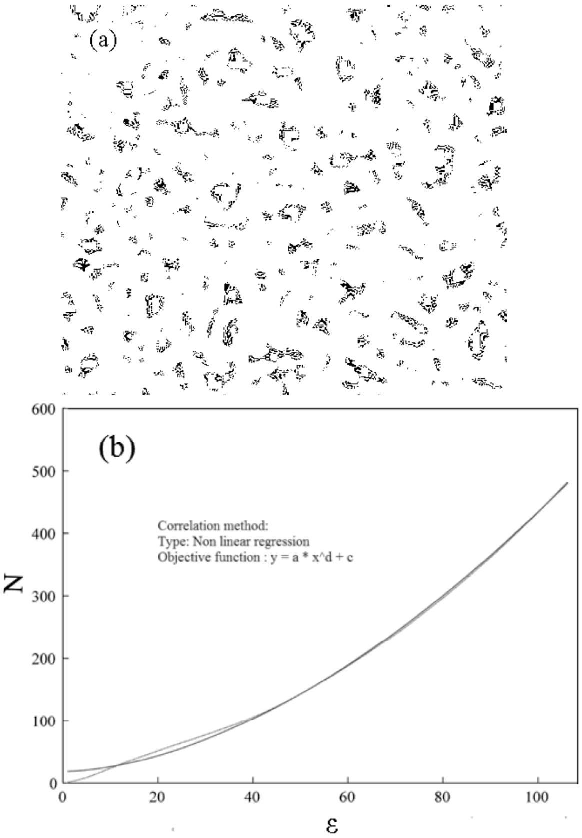

Fig. 2. Fractal morphology of NPC (a) 2-value digital image processed (e.g. 5h), (b) Fitting method for calculating fractal dimension.

of copper, porosity will be formed through the alloy, forming a three-dimensional connectivity of the porous structure (Fig. 1b), and as-dealloyed ribbons have been basic completely corroded. This also has been verified by EDS results. After that, with the diffusion of copper atoms, copper atoms were further agglomerated, resulting in the reduction of the surface area and the increase of the pore size. This is shown in Figs. 1c and 1d. Further corrosion, the porous structure of NPC can be destroyed, highlighted by the arrow in Fig. 1e. Until 17 hours of corrosion time, porous structure almost completely collapsed (Fig. 1f). If the corrosion time is long enough, copper atoms in alloy ribbons will be completely eroded, and the color of the solution finally becomes green.

Fig. 2 shows the process of calculating fractal dimension of NPC's surface that corroded for 5 hours: Fig. 2a is the processed 2-value FE-SEM image, Fig. 2b indicates how the fractal dimension calculated. Fig. 3a illustrates corrosion time dependence of fractal dimension. The calculation of fractal dimension and fitting parameters obtained from the different corrosion time are shown in Table 1. It is seen from Fig. 3a that the values of the fractal dimension (D) of NPC's surface morphology obtained under the different corrosion times in this work are all greater than its topological dimension D_T (D_T = 1). In fractal theory, an irregular or non-Euclidean shape is considered a transition between two regular ones. Therefore, an important indicator of a fractal structure is that its fractal dimension is greater than its topological dimension and less than its Euclidean one. This indicates that the NPC's surface morphology belongs to a kind of fractal structure with fractal dimension of 1.59-1.74 according to the fractal definition presented by Mandelbrot [11]. It is known from the calculation of fractal dimension of NPC's surface morphology obtained under the different corrosion time that all data accord with power law relationship shown in Fig. 2b. The power law relationship further shows that NPC's surface morphology has the fractal characteristic. Thus, fractal dimension as a characteristic parameter can be used to describe NPC's surface morphology. It can see in Fig. 3a that there are three characteristic temporal stages in the evolution of NPC's surface. The application of corrosion time causes enhancing of the surface roughness that is the formation of

Table 1. Fitting parameters of fractal dimension by correlation method.

Corrosion time [h]	FD	*a*	*c*	correlation coef.
2	1.590	0.13569	11.414	0.998218
5	1.740	0.13759	18.294	0.998823
8	1.691	0.13486	30.817	0.988220
11	1.546	0.28267	24.269	0.993532
14	1.484	0.44636	16.020	0.997631
17	1.618	0.14568	18.714	0.996100

deeper holes with simultaneous decaying of relatively flat portions formed (Stage I in Fig. 3a). The increment of the fractal dimension at the first stage characterizes the degree of complexity of holes. After that, fractal dimension drops down to 1.484 (Stage II in Fig. 3a). Further evolution of NPC's surface with corrosion time leads to an insignificant increase of fractal dimension as porous structure almost completely collapsed (Stage III in Fig. 3a). It is worthy to note that the fractality of the processed 2-vaule image is in agreement with the well known self-similarity of mass-number distributions in cluster ensembles. In other words, the morphology gradually transforms from the complicated shape to the simple shape with the corrosion time increasing (Stage III in Fig. 3a). The computing results of fractal dimension of NPC's surface morphology indicate that the value of fractal dimension relates to the complicated extent of the object shape.

Fig. 3b shows the pore size and ligament size as function of corrosion time. As corrosion time increased, pore size and ligament size both increased and then decreased. Mean pore size ranges from 325 nm to 520 nm, minimum pore size 153 nm to 257 nm and maximum pore size 552 nm to 996 nm. Moreover, the ligament size is between 114 nm and 214 nm. Therefore, corrosion time can affect the pore size and ligament size.

4. CONCLUSIONS

In summary, monolithic NPC ribbons can be fabricated by free corrosion dealloying of rapidly solidified $Mn_{70}Cu_{30}$ alloy in a 6 wt.% HCl solution. Moreover, prepared NPC was uniform network-like structure. Different corrosion time have a certain effect on the morphology of NPC's surface, with the average ligament size in the range of 114-214 nm and the average pore size of 325-520 nm. Porous structure of NPC is of typical fractal characteristic with fractal dimension of 1.59-1.74. The computing results of the fractal dimension of NPC's surface morphology indicate that the value of fractal dimension relates to the complicated extent of the object shape.

ACKNOWLEDGEMENTS

The authors would like to acknowledge Natural Science Fundation of China (50871047, 50371047), Natural Science Fundation of Shandong Province (ZR2010ZM071) and the Fund of Innovation Project of Graduate of University of Jinan (YCX10016) with this work.

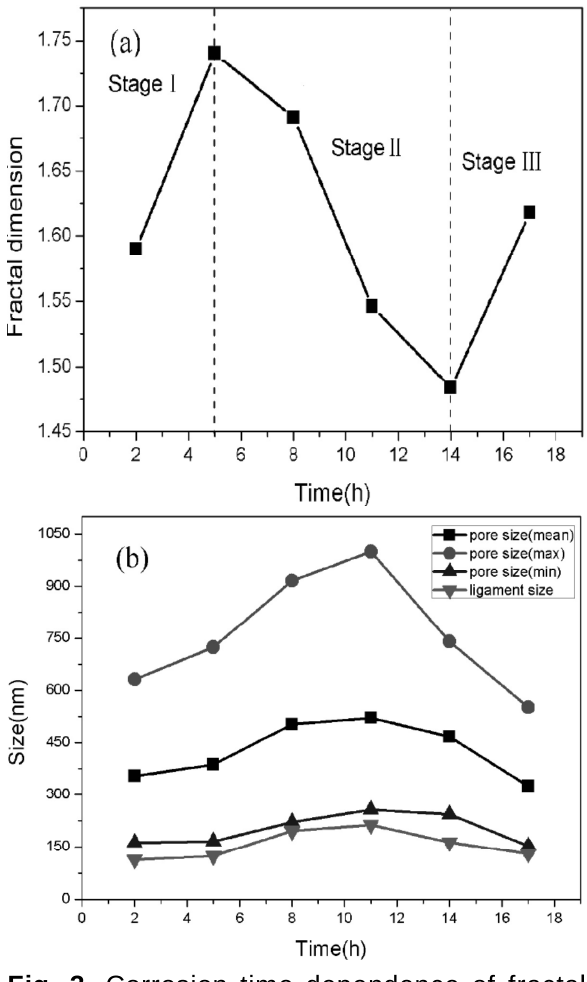

Fig. 3. Corrosion time dependence of fractal dimension (a), pore size and ligament size (b) of NPC.

REFERENCES

[1] G.C. Bond and D.T. Thompson // *Catal. Rev.* **41** (1999) 319.

[2] T. You, O. Niwa, M. Tomita and S. Hirono // *Anal. Chem.* **75** (2003) 2080.

[3] J. Weissmueller, R.N. Viswanath, D. Kramer, P. Zimmer, R. Wuerschum and H. Gleiter // *Science* **300** (2003) 312.

[4] S.H. Joo, S.J. Choi, K.J. Kwa and Z. Liu // *Nature* **412** (2001) 169.

[5] J. Erlebacher, M.J. Aziz, A. Karma, N. Dimitrov and K. Sieradzki // *Nature* **410** (2001) 450.

[6] R. Zeis, T. Lei, K. Sieradzki, J. Snyder and J. Erlebacher // *Journal of Catalysis* **253** (2008) 138.

[7] E. Detsi, M. van de Schootbrugge, S. Punzhin, P. R. Onck and J. T. M. De Hosson // *Scripta Materialia* **64** (2011) 319.

[8] Z.N. Liu, L.H. Huang, L.L. Zhang, H.Y. Ma and Y. Ding // *Electrochimica Acta* **54** (2009) 7286.

[9] J.R. Hayes, A.M. Hodge, J. Biener and A.V. Hamza // *J. Mater. Res.* **10** (2006) 2611.

[10] J. Feder, *Fractals* (Plenum, New York 1988).

[11] B.B. Mandelbrot, *Fractal: Form, Chance and Dimension* (Freeman Press, San Francisco, 1977).